Journal Name

Dynamic Article Links ►

Cite this: DOI: 10.1039/c0xx00000x

www.rsc.org/xxxxxx

ARTICLE TYPE

Multifunctional ScF_3: Ln^{3+} (Ln = Tb, Eu, Yb, Er, Tm and Ho) nano/microcrystals: hydrothermal/solvothermal synthesis, electronic structure, magnetism and tunable luminescence properties

Lili Han[a], Yuhua Wang[a]*, Linna Guo[a], Lei Zhao[a], Ye Tao[b]

Received (in XXX, XXX) Xth XXXXXXXXX 20XX, Accepted Xth XXXXXXXXX 20XX
DOI: 10.1039/b000000x

Figure S1 shows the PLE (black line) and PL (red line) spectra of ScF_3 nanocrystals under UV light. The excitation spectrum shows a broad band ranged from 200 to 400 nm, and their corresponding emission spectrum gives a broad band ranged from 400 to 500 nm. We assign this luminescence to nanocrystal defects.

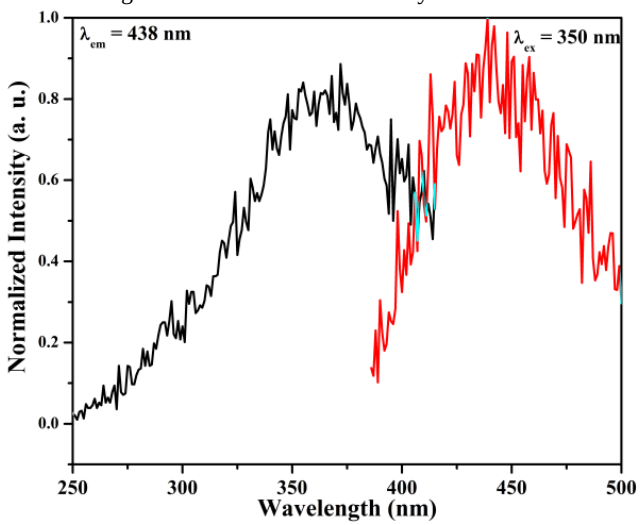

Fig. S1. PLE and PL spectra of ScF_3 nanoparticles under UV light

Fig. S2 shows the PLE (black line) and PL (red line) spectra of the ScF_3 nanocrystals under VUV light. Similarly, the excitation spectrum exhibits a broad band between 125 and 300 nm, and their corresponding emission spectrum shows a band ranged from 300 to 500 nm, which also root in defects in the ScF_3.

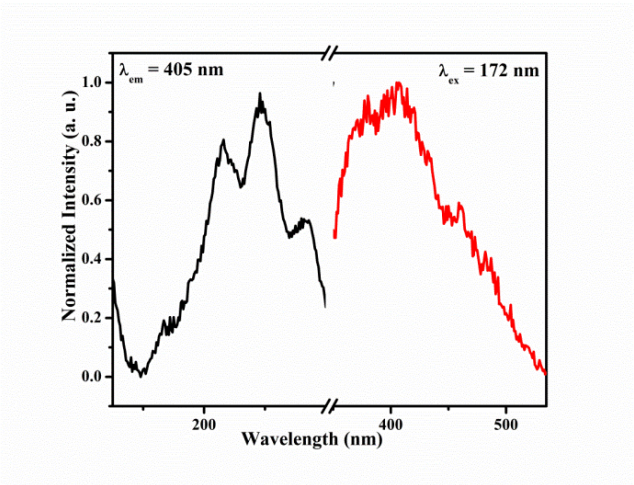

Fig. S2. PLE and PL spectra of ScF_3 nanocrystals under VUV light

Under low-voltage electron-beam excitation (accelerating voltage = 5 kV, filament current = 70 mA), the CL spectrum of ScF_3 nanocrystals gives the characteristic transition of nanocrystal defects.

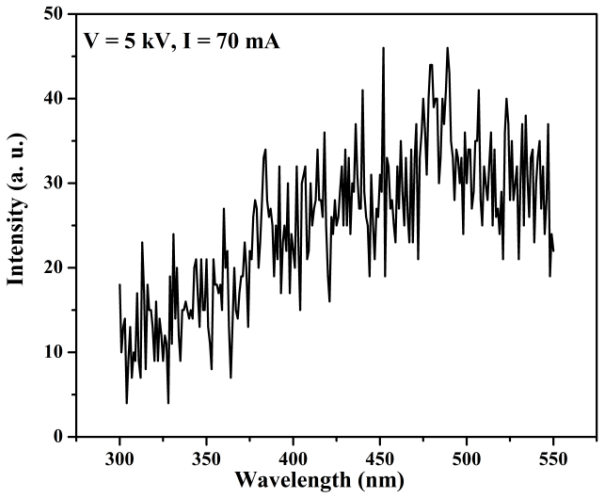

Fig. S3 CL spectra of ScF_3 nanoparticles

It is well known that voltage increases, the carrier transport rate

increases and current increases, the carrier concentration increases. The carrier transport rate or the carrier concentration increases, the higher is the conductivity, and the stronger is the emission. Accordingly, it is reasonable that there is no obvious saturation effect. The increase in CL brightness with an increase in electron energy and filament current is attributed to the deeper penetration of the electrons into the phosphor body and the larger electron-beam current density. The electron penetration depth can be estimated using the empirical formula[1]:

$$L[\text{Å}] = 250\left(\frac{A}{\rho}\right)\left(\frac{E}{\sqrt{Z}}\right)^{n}, n = \frac{1.2}{1-0.29\lg Z}$$

Where A is the atomic or molecular weight of the material, r is the bulk density, Z is the atomic number or the number of electrons per molecule in the compounds, and E is the accelerating voltage (kV). For ScF_3 host, Z = 48, A =101.95, ρ = 2.620 g/ cm^3. So according to the above empirical formula, the estimated electron penetration depths at 1, 2, 3, 4, 5 and 6 kV are about 0.11, 0.56, 1.45, 2.84, 4.78 and 7.32 nm, respectively. For CL of the above samples, the Tb^{3+} ions are excited by the plasma produced by the incident electrons.

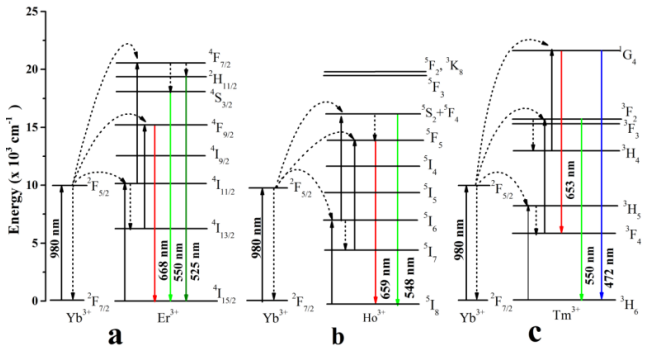

Fig. S4 Energy-level scheme and various observed emission processes in (a) Yb^{3+}–Er^{3+},(b)Yb^{3+}–Ho^{3+} and(c) Yb^{3+}–Tm^{3+} co-doped ScF_3 samples under 980 nm laser diode excitation

The possible mechanism for multi-photon process for Yb^{3+}–Er^{3+}, Yb^{3+}–Ho^{3+} and Yb^{3+}–Tm^{3+} co-doped ScF_3 samples with the energy-level scheme are discussed in detail and shown as follows: (1) For ScF_3: 0.1Yb^{3+}, 0.001Er^{3+}, UC green and red emissions are via two photon processes, as shown in the Fig. S4a. Yb^{3+} initially absorbs a 980 nm photon from the laser source and subsequently transfer the energy to a nearby Er^{3+}, exciting Er^{3+} to the $^4I_{11/2}$ level, then a second 980 nm photon or ET from Yb^{3+} can populate the $^4F_{7/2}$ level of Er^{3+}, afterward Er^{3+} will relax nonradiatively to the $^2H_{11/2}$ or $^4S_{3/2}$or $^4F_{9/2}$ levels, finally resulting in the green ($^2H_{11/2}$, $^4S_{3/2}$) / $^4I_{15/2}$ and red $^4F_{9/2}$ / $^4I_{15/2}$ emissions. In addition, the $^4F_{9/2}$ level may also be populated from the $^4I_{13/2}$ level of Er^{3+} by absorbing a 980 nm photon or ET from Yb^{3+}, with the $^4I_{13/2}$ state being initially populated via nonradiative $^4I_{11/2}$ / $^4I_{13/2}$ relaxation[2-5]. (2) Synchronously, in ScF_3: 0.1Yb^{3+}, 0.001Ho^{3+}, the main UC mechanism for Yb^{3+}-Ho^{3+} pairs in this host is a two photon process depicted in Fig. S4b. Firstly, the ground state electrons of $^5I_8$ are excited to $^5I_6$ of Ho^{3+} through the ET from Yb^{3+}. Some electrons on $^5I_6$ are excited to $^5S_2$/$^5F_4$ through the ET from a second 980 nm photon, generating the green emission of $^5S_2$/$^5F_4$-$^5I_8$ at 548 nm. In addition, the $^5F_5$ level may also be populated from the $^5I_7$ level of Ho^{3+} by absorbing a 980 nm photon or energy transfer from Yb^{3+}, generating the red emission of $^5F_5$-$^5I_8$. The nonradiative relaxation of $^5S_2$/$^5F_4$-$^5F_5$ is the other path for populating the $^5F_5$ level to emit red light [6, 7]. (3) The producing of blue (472 nm), green (550 nm) and red (653 nm) emissions of Tm^{3+}-Yb^{3+} in ScF_3 involve of 3, 2 and 3 photons of 980 nm. As depicted in Fig. S4c, under the 980 nm excitation, Yb^{3+} are firstly excited from the $^2F_{7/2}$ ground state to the $^2F_{5/2}$ excited state, then it can promote an electron from $^3H_6$ to $^3H_5$, and Tm^{3+} at $^3H_5$ relaxes nonradiatively to $^3F_4$. The Tm^{3+} in the $^3F_4$ excited states also can absorb the energy from another Yb^{3+}, leading to the Tm^{3+} at $^3F_4$ transits to $^3F_2$, then decays nonradiatively to $^3H_6$ with a green emission at 550 nm. At the same time, some Tm^{3+} decay from $^3F_2$ to $^3H_4$ states, which can be excited by a subsequent Yb^{3+}, the Tm^{3+} at $^3H_4$ is excited to $^1G_4$, and then finally decays nonradiatively to the $^3H_6$ and $^3F_4$, producing blue emission and red emission at 472 and 653 nm, respectively [8-10].

Notes and references

[a] *Department of Material Science, School of Physical Science and Technology, Lanzhou University, Lanzhou 730000, China*
[b] *Laboratory of Beijing Synchrotron Radiation, Institute of High Energy Physics, Chinese Academy of Sciences, Beijing 100049, China*

1 F. L. Zhang, S. Yang, C. Stoffers, J. Penczek, P. N. Yocom, D. Zaremba, B. K. Wagner and C. J. Summers, *Appl. Phys. Lett.*, 1998, **72**, 2226.
2 D. Li, B. Dong, X. Bai, Y. Wang and H. W. Song, *J. Phys. Chem. C*, 2010, **114**, 8219.
3 X. G. Yu, Y. Shan, G. C. Li and K. Z. Chen, *J. Mater. Chem.*, 2011, **21**, 8104
4 D. K. Ma, D. P. Yang, J. L. Jiang, P. Cai and S. M. Huang, *CrystEngComm.*, 2010, **12**, 1650
5 D. Manzani, J. L. Ferrari, F. C. Polachini, Y. Messaddeq and S. J. L. Ribeiro, *J. Mater. Chem.*, 2012, **22**, 16540
6 N. Niu, F. He, S. L. Gai, C. X. Li, X. Zhang, S. H. Huang and P. P. Yang, *J. Mater. Chem.*, 2012, **22**, 21613
7 B. Zhou, L. L. Tao, Y. H. Tsang and We. Jin, *J. Mater. Chem. C*, 2013, **1**,4313
8 X. Bai, D. Li, Q. Liu, B. Dong, S. Xu and H. W. Song, *J. Mater. Chem.*, 2012, **22**, 24698
9 S. H. Huang,X. Zhang, L. Z. Wang, L. Bai, J. Xu, C.X. Li and P. P. Yang, *Dalton Trans.*, 2012, **41**, 5634
10 F. Wang and X. G. Liu, *Chem. Soc. Rev.*, 2009, **38**, 976